Precambrian Research 174 (2009) 145–154

Contents lists available at ScienceDirect

Precambrian Research

journal homepage: www.elsevier.com/locate/precamres

# Validating the existence of Vaalbara in the Neoarchean

Michiel O. de Kock[a,*], David A.D. Evans[b], Nicolas J. Beukes[a]

[a] Department of Geology, University of Johannesburg, Auckland Park 2006, South Africa
[b] Department of Geology and Geophysics, Yale University, New Haven, CT 06511, USA

ARTICLE INFO

*Article history:*
Received 20 February 2009
Received in revised form 26 June 2009
Accepted 7 July 2009

*Keywords:*
Paleomagnetism
Continental Reconstruction
Kaapvaal
Pilbara
Neoarchean

ABSTRACT

An interesting aspect of Precambrian geology is the similarities between successions of the Kaapvaal and Pilbara cratons of southern Africa and Australia. Coeval trends in these successions are commonly used to reconstruct global atmospheric and oceanic conditions during the Archean-Proterozoic transition. The similarities, however, could also suggest their paleogeographic proximity in the form of a supercraton, or even Earth's oldest assembled continent, named Vaalbara. If these cratons indeed were nearest neighbours in a supercraton, the parallel trends preserved in supracrustal sequences may reflect local effects in a single basin instead of global paleoenvironmental conditions. Here we report a paleomagnetic pole from the Neoarchean Ventersdorp Supergroup of South Africa, which provide quantitative support for Vaalbara's existence. Our reconstruction differs greatly from earlier suggestions and contests those that place the cratons far apart. It provides the oldest example, and the only Archean instance, of paleomagnetic reconstruction between continental blocks in terms of paleolatitude and relative longitude. If correct, our reconstruction implies that previous paleoenvironmental conclusions may need reconsideration.



## 1. Introduction

The existence of a Vaalbara supercraton or early continent is suggested by similarities in stratigraphic elements between the Kaapvaal and Pilbara cratons. In particular are those regarding Paleoproterozoic iron-formations (Trendall, 1968), but there are also broader links between 3.5 Ga and 1.8 Ga volcano-sedimentary basins and mineral deposits (e.g., Button, 1979; Cheney, 1996). Some ascribe the similarities to global processes (e.g., Nelson et al., 1999) and question Vaalbara's existence. An alternative reconstruction, named Ur (Rogers, 1996), places the cratons far apart, thus imposing global controls on the parallel trends. In this way the correlation of sulphur isotopic data between the cratons have been interpreted to reflect global changes linked to atmospheric evolution (Kaufman et al., 2007). The Ur hypothesis, which places the cratons in their Gondwanaland configuration (Rogers, 1996), is contradicted by widespread evidence of Precambrian collisional orogens between Australia and Africa (e.g., Fitzsimons, 2000; Boger et al., 2001; Meert, 2003; Jacobs and Thomas, 2004; Collins and Pisarevsky, 2005); yet it has continued to receive support and mention in the literature (e.g., Mukherjee and Das, 2002; Rogers and Santosh, 2003; Zhao et al., 2006). Confusingly Mondal et al. (2009) depicts what they call an "Ur" protocontinent at 2400–2200 Ma in which the Pilbara and Kaapvaal cratons are placed within a more traditional Vaalbaran configuration. A plethora of suggested reconstructions, some going under the same name, and disagreement among authors about which one is more credible at any specific time, all create confusion in the geosciences community. In this paper we test the various reconstructions involving the Kaapvaal and the Pilbara cratons during the Neoarchean, with the goal of eliminating some and providing more credence to others.

In Vaalbara, Pilbara is traditionally juxtaposed next to the southwestern margin of the present-day Kaapvaal craton (Cheney, 1996). This is referred to hereafter as the "Cheney" fit. Cheney included the Zimbabwe and the Yilgarn cratons in their present configurations relative to the Kaapvaal and Pilbara cratons in his definition of Vaalbara (Cheney, 1990, 1996). The Grunehogna craton of Antarctica, positioned in a Mesozoic Gondwana reconstruction (Jones et al., 2003), can also be included.

A paleolatitude comparison at 2.78–2.77 Ga at first failed to lend support for Vaalbara's existence (Wingate, 1998), but with updated Pilbaran poles (Strik et al., 2003), a direct juxtaposition became allowable. Another set of older Neoarchean poles (Zegers et al., 1998), but with large associated age uncertainties, also allow Pilbara–Kaapvaal proximity. By placing Pilbara towards the east of Kaapvaal ("Zegers" fit) a fair alignment of Archean structural elements is achieved. Since the paleomagnetic method of single-age pole comparison, as used by Zegers and Strik (see previous citations), does not provide relative longitudinal constraints, it is equally allowable that the cratons were far apart along their respective bands of paleolatitude. They may also have been in opposite hemispheres due to geomagnetic polarity ambiguity.

* Corresponding author. Tel.: +27 115594707; fax: +27 115594702.
*E-mail address:* mdekock@uj.ac.za (M.O. de Kock).

0301-9268/$ – see front matter © 2009 Elsevier B.V. All rights reserved.
doi:10.1016/j.precamres.2009.07.002

We report a new paleopole for the ~2.7 Ga Ventersdorp Supergroup of South Africa that, together with existing data (Wingate, 1998), allow for the comparison of distances between paleopoles from both cratons through a better constrained time interval (i.e., 2.78–2.70 Ga), using two pairs of coeval poles from the two blocks. This provides relative paleolongitudinal constraints for a more uniquely determined reconstruction.

## 2. Ventersdorp–Fortescue correlation

The Ventersdorp Supergroup is the most extensive volcano-sedimentary sequence on the Kaapvaal craton and is largely undeformed and very well preserved, having only reached lower greenschist facies (Crow and Condie, 1988). It is lithostratigraphically (e.g., Wingate, 1998) and chemically (Nelson et al., 1992) very similar to the Fortescue Group of Australia, but a simple correlation is unsupported by published age data (Fig. 1). The Fortescue Group, which has been densely sampled for geochronology, dates from 2772 ± 2 Ma (Wingate, 1999) to 2713 ± 3 Ma (Blake et al., 2004), and by current estimates appears to be mostly older than the Ventersdorp Supergroup. A 2714 ± 14 Ma age for basalt at the base of the Ventersdorp (Armstrong et al., 1991), however, remains unverified, and it could conceivably be as old as 2764 ± 5 Ma (England et al., 2001), the maximum age for the underlying Witwatersrand Supergroup. If this is so, the Klipriviersberg Group would be analogous to the Mt. Roe Basalt of Australia and the Derdepoort volcanics and Kanye volcanics from the northwestern Kaapvaal craton, dated at 2772 ± 2 Ma (Wingate, 1999), 2781 ± 5 Ma (Wingate, 1998), and 2784 ± 2 Ma (Grobler and Walraven, 1993; Moore et al., 1993), respectively.

The 2709 ± 8 Ma age for bimodal volcanic rocks overlying the Klipriviersberg Group (Armstrong et al., 1991) is accepted even though lithostratigraphic equivalents on the western margin of the craton yield older U-Pb ages (de Kock, 2007; Poujol et al., 2005), and the age of the Allanridge Formation, although not directly dated, is fairly well constrained. The Allanridge lies unconformably between one sequence dated at 2709 ± 8 Ma and another dated at 2664 ± 6 Ma (Barton et al., 1995), thus making it comparable, within uncertainties, to the ~2713 Ma Maddina Basalt of Australia (Fig. 1).

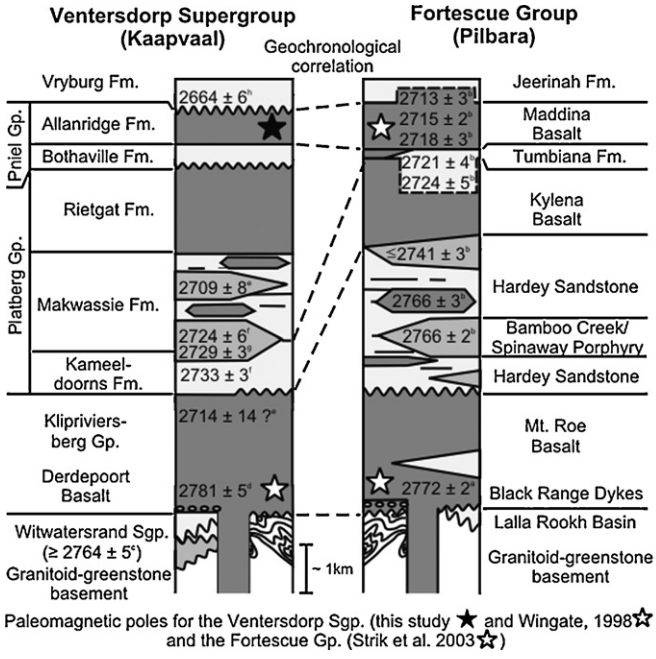


**Fig. 1.** Correlation of the Ventersdorp Supergroup and the Fortescue Group. Diagram is modified after Wingate (1998). Age references: (a) Wingate (1999), (b) Blake et al. (2004), (c) England et al. (2001), (d) Wingate (1998), (e) Armstrong et al. (1991), (f) de Kock (2007), (g) Poujol et al. (2005) and (h) Barton et al. (1995).

To complement the 2781 ± 5 Ma Derdepoort pole (Wingate, 1998), and to achieve our proposed double pole-pair comparison, we conducted a paleomagnetic study of the Allanridge Formation. Previous paleomagnetic work (Jones et al., 1967; Henthorn, 1972; Strik et al., 2007) either pre-date the use of progressive demagnetization techniques or lack adequate stability field tests.

## 3. New paleomagnetic data

### 3.1. Sampling sites and laboratory techniques

Table 1 provides a summary of sampling sites, their localities, lithologies sampled and bedding attitude associated with each. All samples were drilled in the field with a portable, hand-held gasoline-powered drill. A magnetic compass, and for most samples also a sun compass, were used for orientation. Individual cores were trimmed to one or more specimens 2.4 cm in length.

At Taung the Allanridge Formation was sampled at three sites. At Ritchie, two lava flows separated by a prominent amygdaloidal flow-top were sampled. A total of eleven sites were sampled along exposures cut by the Orange River between the towns of Hopetown and Douglas (see Fig. 2 for the geological setting of these sampling localities). In addition two compound or sheet flows and a blocky flow-top breccia, pillow flows and pillow fragments in volcanic breccias were extensively sampled along the Orange River.

Andesitic lava samples were prepared using standard methods and were subjected to magnetic cleaning, which consisted of low-field-strength alternating-field (AF) pre-treatment and stepwise thermal demagnetization to 580 °C. Measurements were made with an Agico JR6-A spinner magnetometer within a magnetically shielded room at the University of Johannesburg, South Africa. Alternating-field demagnetization was carried out with a Molspin 2-axis tumbling demagnetizer and thermal demagnetization, in a shielded furnace. Calculation of paleomagnetic poles assumes an axial-geocentric dipolar magnetic field and a paleoradius for the Earth equal to the present Earth radius.

Magnetic components were identified and quantified via least squares principal component analysis (Kirschvink, 1980). These calculations, together with all subsequent statistical analyses, utilized software Paleomag (Jones, 2002), PaleoMac (Cogné, 2003) and the PmagPy open source software by Lisa Tauxe.

### 3.2. Results

Stable and consistent magnetic components were identified in all but one site, which displayed an erratic distribution of components. In addition to low-coercivity and present local field-like components (PLF for short), demagnetization revealed up to three higher-stability components (A, B+ and B−). Samples usually recorded two components, but never all three (Fig. 3 and Table 2).

Six sites revealed northerly and downward-directed components (A) within the temperature range of 375–450 °C, but sometimes persisting up to 500 °C. In most cases, however, demagnetization above 450 °C revealed characteristic components (B+ or B−). Sample magnetization became irregular above 540 °C. Characteristic components were southerly and steeply downward-directed (B+) in 88% of the sites, while one site revealed opposite polarity components (i.e., north and up or B− for short). B+ and B− are not strictly antipodal, but this is unsurprising as the B− component falls within a cloud of normal data that is undersampled in this instance by our one site.

**Table 1**
Summary of sampling site information.

| Site | Locality (°N, °E) | *N* | Lithology | Bedding (strike/dip) |
|---|---|---|---|---|
| Taung | | | | |
| TGC | −27.15°, 024.78° | 14 | Massive lava | 152°/10°SW |
| TGD | −27.53°, 024.85° | 12 | Massive lava | 262°/12°NW |
| TGE | −27.54°, 024.84° | 7 | Porphyritic lava | Sub-horizontal |
| Ritcie | | | | |
| RCBa | −29.04°, 024.56° | 20 | Amygdaloidal lava | Sub-horizontal |
| RCBb | −29.04°, 024.56 | 3 | Amygdaloidal lava | Sub-horizontal |
| Hopetown-Douglas | | | | |
| HTA | −29.57°, 024.08° | 41 | Pillow lava and pillow clasts | Sub-horizontal |
| HTB | −29.57°, 024.07° | 26 | Pillow lava, clasts and hyaloclastite matrix | Sub-horizontal |
| HTC | −29.48°, 023.94° | 18 | Amygdaloidal lava | Sub-horizontal |
| HTDa | −29.30°, 023.81° | 7 | Amygdaloidal lava | Sub-horizontal |
| HTDb | −29.30°, 023.81° | 6 | Amygdaloidal lava | Sub-horizontal |
| HTDc | −29.30°, 023.81° | 6 | Blocky flow-top breccia clasts | Sub-horizontal |
| HTE | −29.29°, 023.82° | 13 | Massive lava | 194°/9°W |
| HTF | −29.39°, 023.93° | 15 | Porphyritic lava | 191°/9°W |
| HTG | −29.39°, 023.92° | 17 | Massive lava | Sub-horizontal |
| HTH | −29.48°, 023.93° | 6 | Amygdaloidal lava | Sub-horizontal |
| HTI | −29.48°, 023.93° | 10 | Amygdaloidal lava | Sub-horizontal |

*N* = number of samples taken at each site.

### 3.3. Intraformational conglomerate tests

Hyaloclastite clasts and interbedded pillow flows provide an opportunity for conducting a conglomerate test (Fig. 4a). A second test was performed on clasts from a flow-top breccia (Fig. 4b). Pillow fragments, of variable internal texture, displayed similar behaviour to that of underlying and overlying pillow lavas during low level demagnetization (Fig. 4a). Low-coercivity components were removed in all of the samples and PLF components in 65% of the pillow fragment samples. At higher demagnetization levels (i.e., above 300 °C), samples displayed linear trajectories towards the origin. These characteristic components, however, have a scattered distribution and differ significantly from the underlying and overlying pillow flows, which displayed well-grouped B+ components at similar demagnetization levels (Fig. 4a). A suite of statistical tests demonstrates (see below) that the distribution of character-

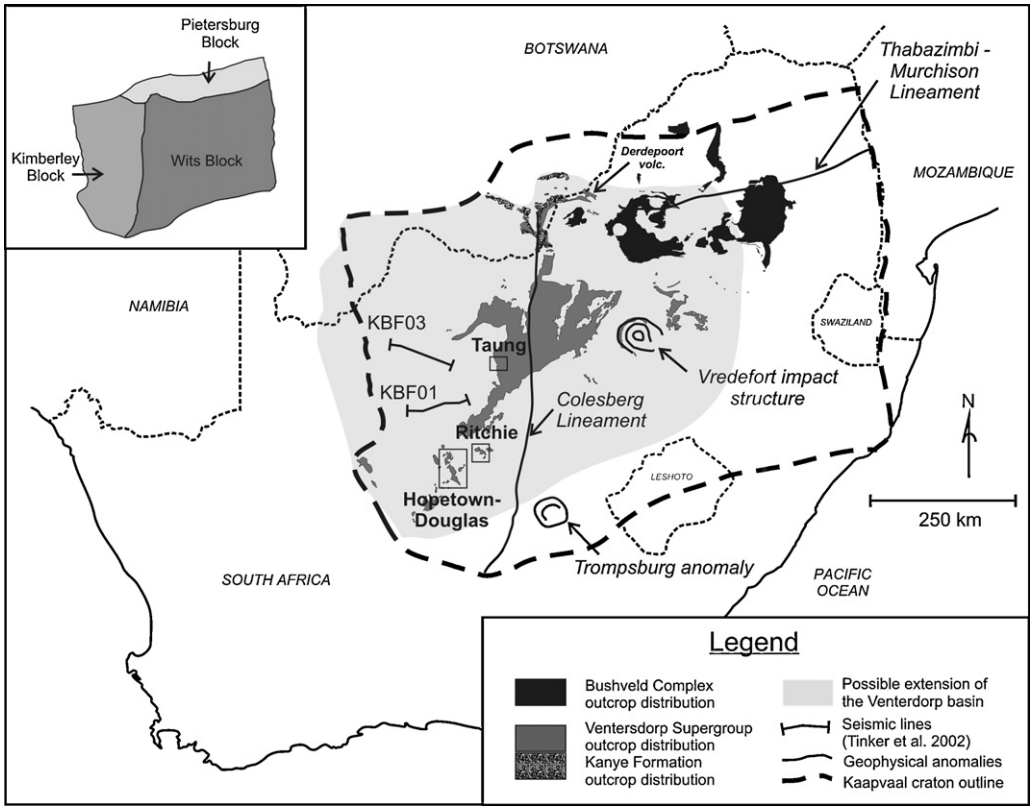


**Fig. 2.** Geological setting of sampling areas at Taung, Ritchie and between Hopetown and Douglas. Outcrop distribution of the Ventersdorp, the Kanye Formation and the Bushveld Complex are simplified from geological maps of South Africa (Council for Geoscience, 1997) and Botswana (Geological Survey Department Lobatse, 1984). Geophysical outlines of the craton, the Trompsburg anomaly and the Vredefort impact structure as well as major crustal elements (i.e., the Thabazimbi-Murchison lineament and the Colesberg lineament) were identified from an aeromagnetic map produced by De Beers (1998). The seismic lines provide information on the possible extent of the Ventersdorp basin. Insert depicts crustal blocks (De Beers, 1998; Eglington and Armstrong, 2004).

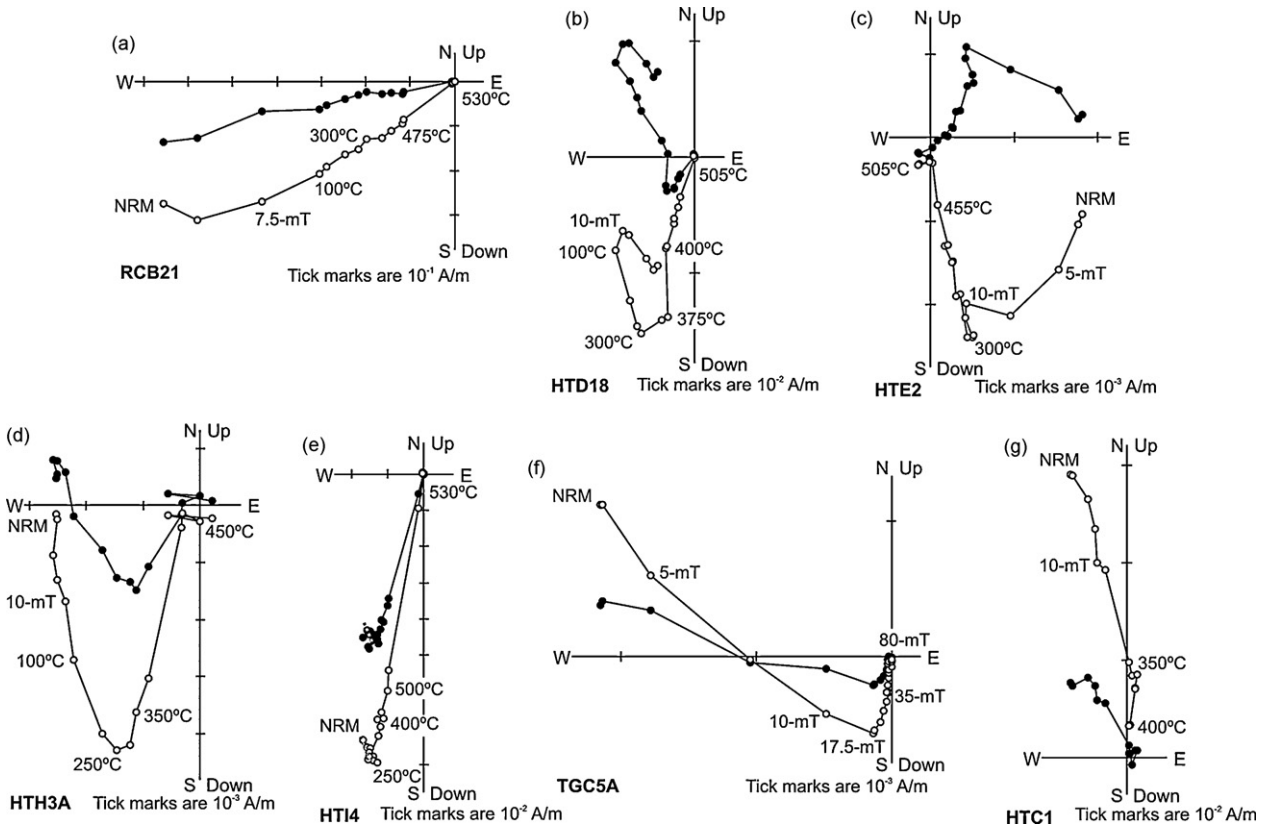


**Fig. 3.** Representative sample demagnetization behaviour. (a) Some samples did not respond well to demagnetization due to the adverse affects of lightning strikes, these samples record high-coercivity components of random orientation. (b–f) Apart from inconsistent low-coercivity components and local present-field-like (PLF) components, some samples (plot b) displayed intermediate temperature northerly and down directed or A-components, while most samples (plots b–e and f, respectively) displayed either high-stability southerly downward (B+) or northerly and upward (B−) directions. Solid symbols = horizontal plane, open symbols = E-W and vertical plane. NRM = natural remanent magnetization.

istic directions in the fragments is significantly distinct from that of the lava flows. This represents a positive intraformational conglomerate test and supports a conclusion that the B+ remanence is primary. In further support of this, characteristic components derived from a pair of individually oriented core samples from one pillow differ significantly from B+ directions seen in other pillows around it (Fig. 4a). The presence of coherent PLF components in these samples and the surrounding pillows excludes orientation error (Fig. 4a), and the most plausible explanation is that the sampled pillow represents a rotated body that became reconsolidated in the pillow lava hyaloclastite-unit.

A flow-top breccia was sampled at a locality about 46 km northwest of the pillow lava hyaloclastite-unit. The breccias from this locality is a lenticular unit at the top-edge of and underlying lava

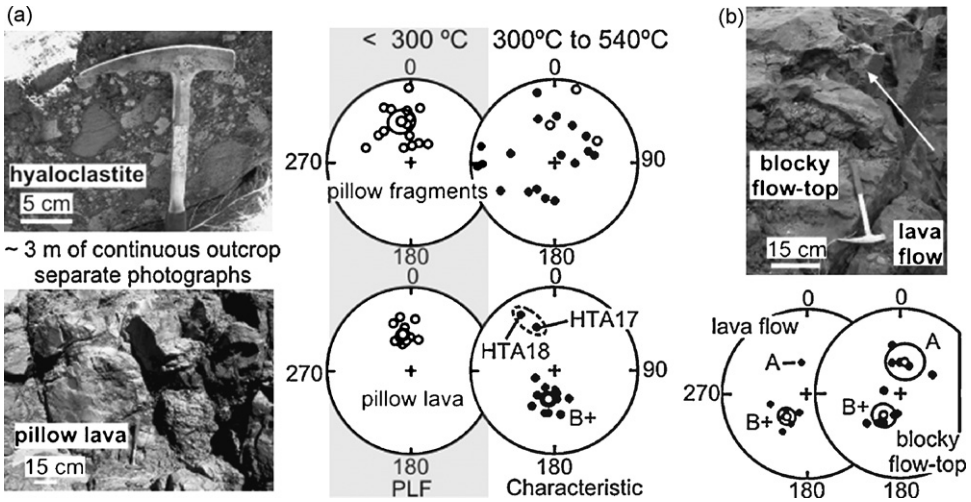


**Fig. 4.** Intraformational conglomerate tests. Equal-area plots: solid = lower hemisphere, open = upper hemisphere, grey filled symbol and ellipse = component mean and associated 95% cone of confidence. (a) Positive test for pillow lava (bottom) and hyaloclastite clasts (top). Components below 300 °C (PLF) and those at higher demagnetization levels (characteristic components) are shown. Samples HTA18 and 17 originate from the same rotated pillow. (b) Negative test for components A and B+ in a lava flow and an associated blocky flow-top. Arrow in photo = stratigraphic up.

**Table 2**
Summary of least-squares component directions and component means for the Allanridge Formation.

| Site | *n*/*N* | *L*/*P* | Unbl. | Declination | Inclination | *K* | $\alpha_{95}$ |
|---|---|---|---|---|---|---|---|
| PLF components | | | | | | | |
| TGE | 5/7 | 5/0 | 300 °C | 006.6 | −54.4 | 39.3 | 12.4 |
| RCBa | 6/20 | 6/0 | 200 °C | 317.7 | −52.0 | 21.3 | 14.9 |
| HTA | 14/18 | 14/0 | 300 °C | 348.0 | −53.2 | 42.8 | 5.7 |
| HTA (clasts) | 15/23 | 15/0 | 200 °C | 346.4 | −51.4 | 10.5 | 12.4 |
| HTB | 10/15 | 10/0 | 200 °C | 339.7 | −58.4 | 45.9 | 7.2 |
| HTB (matrix) | 6/7 | 6/0 | 200 °C | 027.6 | −59.6 | 12.4 | 19.8 |
| HTC | 15/18 | 15/0 | 300 °C | 328.8 | −58.8 | 25.2 | 8.1 |
| HTDc | 5/6 | 5/0 | 300 °C | 341.7 | −58.2 | 17.8 | 18.6 |
| THE | 11/13 | 11/0 | 250 °C | 334.2 | −51.1 | 42.1 | 7.1 |
| HTF | 3/15 | 3/0 | 300 °C | 328.8 | −60.5 | 75.9 | 14.2 |
| HTG | 13/15 | 13/0 | 250 °C | 334.6 | −57.9 | 43.0 | 6.4 |
| HTH | 6/6 | 6/0 | 250 °C | 335.2 | −56.6 | 144.3 | 5.6 |
| HTI | 9/10 | 9/0 | 300 °C | 340.0 | −53.3 | 41.1 | 8.1 |
| | | | PLF mean | 341.7 | −56.9 | 63.2 | 5.3 |
| North down components | | | | | | | |
| RCBa | 9/20 | 9/0 | 450 °C | 314.6 | 63.6 | 28.7 | 9.8 |
| HTDc | 5/6 | 5/0 | 375 °C | 008.6 | 58.7 | 18.7 | 18.1 |
| THE | 8/13 | 8/0 | 375 °C | 359.4 | 58.0 | 14.1 | 15.3 |
| | | | North down mean | 349.7 | 62.0 | 33.7 | 21.6 |
| Characteristic components (south down) | | | | | | | |
| TGC[a] | 14/14 | 14/0 | 450 °C | 198.5 | 47.2 | 30.1 | 7.4 |
| TGE | 5/7 | 3/2 | 520 °C | 158.9 | 65.6 | 24.8 | 16.8 |
| RCBa | 13/20 | 13/0 | 540 °C | 221.5 | 74.5 | 63.2 | 5.3 |
| HTA | 14/18 | 14/0 | 500 °C | 191.8 | 61.1 | 31.9 | 7.2 |
| HTB | 13/15 | 10/3 | 500 °C | 184.2 | 68.4 | 12.5 | 12.3 |
| HTDa | 6/7 | 5/1 | 490 °C | 215.8 | 62.0 | 86.0 | 7.4 |
| HTDb | 4/6 | 3/1 | 490 °C | 236.2 | 55.2 | 30.8 | 17.8 |
| HTDc | 5/6 | 5/0 | 490 °C | 213.0 | 60.6 | 40.2 | 12.2 |
| HTE[a] | 5/13 | 3/2 | 515 °C | 213.0 | 63.8 | 52.3 | 11.4 |
| HTF[a] | 15/15 | 15/0 | 550 °C | 216.1 | 58.3 | 59.6 | 5.0 |
| HTG | 15/15 | 14/1 | 550 °C | 199.9 | 66.4 | 23.5 | 8.1 |
| HTH | 6/6 | 6/0 | 470 °C | 198.2 | 62.6 | 113.7 | 6.3 |
| HTI | 9/10 | 9/0 | 555 °C | 195.7 | 58.4 | 217.7 | 3.5 |
| | | | South down mean | 203.9 | 62.5 | 88.6 | 4.9 |
| Characteristic components (north up) | | | | | | | |
| HTC | 7/18 | 5/2 | 440 °C | 4.5 | −85.1 | 75.0 | 7.2 |

*n*/*N* = number of samples included/number analyzed, *L*/*P* = line versus plane least squares analyses, Unbl. = temperature in degrees Celsius at which component unblocks, declination = mean declination in degrees, inclination = mean inclination in degrees, *k* = Fisher's precision parameter, except when in modified form for where both line and plane data were combined, and $\alpha_{95}$ = radius of 95% confidence cone about the mean.

[a] Sites for which bedding corrections were applied.

flow, and it resembles a flow toe. At a maximum it is about 3 m thick, but it pinches out towards the east in less than 5 m. The breccia unit grades laterally westward as well as downward into massive andesitic lava (of which there is ∼4 m thickness exposed) with irregular amygdale-rich zones. Another massive lava unit with patchy amygdale zones wrap across and overlie the sampled breccia-lavaflow unit (a maximum of 2 m thickness of this overlying unit is exposed). Demagnetization of flow-top breccia clasts clearly suggests that the acquisition of medium-temperature A and the characteristic B+ components occurred after fragmentation (Fig. 4b). We suggest that the longer cooling time of the flow-top unit stands in contrast to the quenching of the pillow clasts and shards in the hyaloclastite, and further suggest that, in this case, B+ was acquired shortly after fragmentation and during cooling of the lava-breccia-unit. Another possibility is that it represents a remagnetization acquired during post-depositional re-heating and cooling due to an overlying flow unit. We are cautious in our interpretation given the limited exposure of the overlying flow unit. We do, however, interpret remanence A to be a much younger magnetic overprint. A is better developed in the blocky flow-top compared to the parent lava flow (Fig. 4b), and we propose that the higher permeability of the breccia made it more prone to alteration and later magnetic overprinting.

### 3.3.1. Statistical evaluation of the conglomerate test HTA

In contrast to the well-grouped south-down characteristic directions within pillow lava samples, those identified in fragments of pillow lava are significantly more scattered when viewed on a stereographic projection (Fig. 4a). The majority of these scattered directions (i.e., 18 out of 21 clasts) are positively inclined and about five resemble the south-down character of the components from the parent lithology. This may explain why the Watson's test for randomness fails ($R = 10.91 > R_0 = 7.40$ for $n = 21$). The Shipunov conglomerate test (Shipunov et al., 1998), which employs alternative hypothesis testing, passes if the present local geomagnetic-field (PLF) direction is used as a known secondary overprint ($\rho = -0.259 < \rho_c = 0.207$). We interpreted this to mean that demagnetization procedure adequately removed the PLF overprint (which is apparent from Zijderveld diagrams), but we are not satisfied to reject the possibility that the characteristic components are non-random. A perhaps more meaningful implementation of the Shipunov test would be to use the south-down direction as a potential regional overprint direction. Upon doing so, the test becomes negative ($\rho = 0.351 > \rho_c = 0.207$). This suggests that the south-down direction is present in some of the clasts. We are, however, still wary of rejecting the randomness of the dataset for several reasons. The suite of clast directions is visually distinct from that of the par-

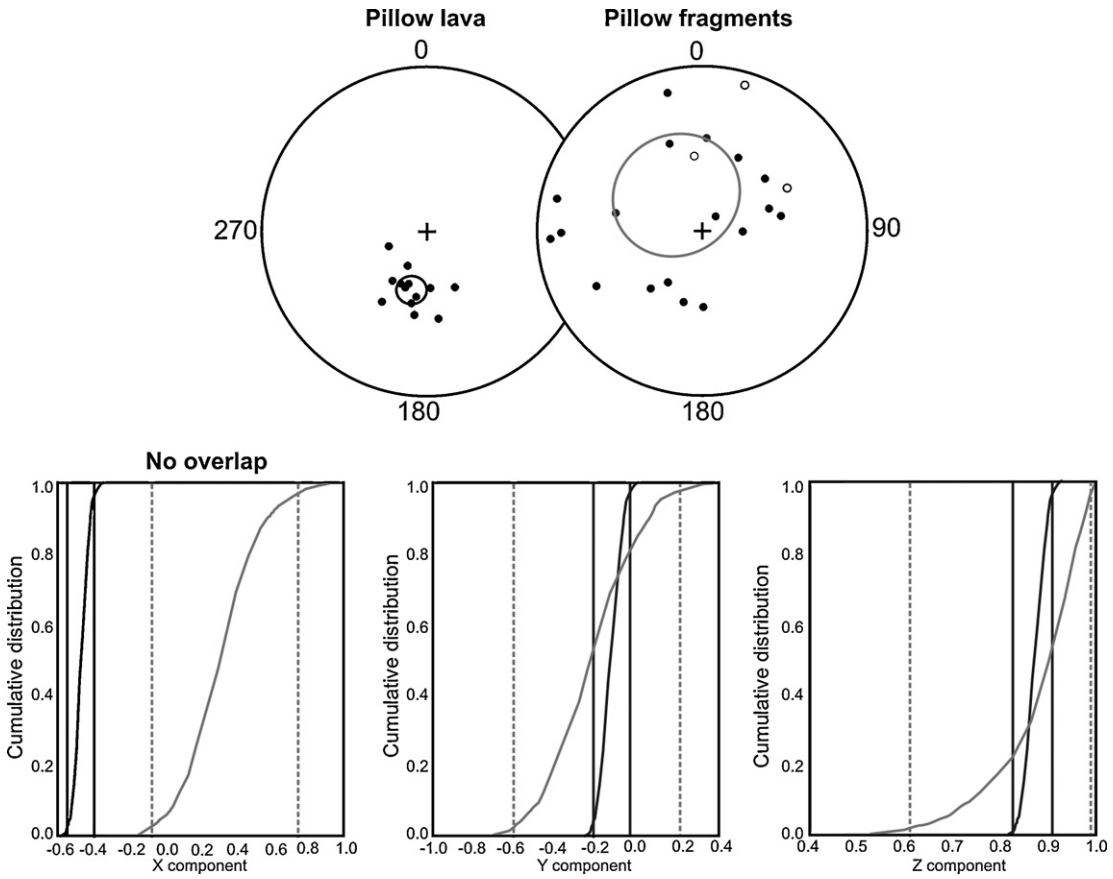


**Fig. 5.** Test for common (Tauxe et al., 2009) mean showing that the two data sets do not share a common mean. Top panel shows equal area projections of characteristic remanence directions from pillow lava (left) and pillow fragments (right) and their associated mean values and 95% confidence cones. Open symbols = upper hemisphere, closed symbols = lower hemisphere. Bottom panels show cumulative distributions of component means in cartesian coordinates. Solid black = pillow fragments and 95% confidence as solid vertical lines, solid grey = pillow samples and 95% confidence as stippled vertical lines. There is no overlap between the distributions of the *x*-components of the pillow lava samples and that of the pillow fragment samples, suggesting that the two data sets do not share a common mean.

ent lithology, while exhibiting similar demagnetization behaviour. There is therefore reason to believe that the null-hypothesis is true (i.e., the dataset is random) despite indications that the alternative hypothesis is true (south-down direction is present). Rejecting the null-hypothesis would result in a Type-1 error. Furthermore, the Shipunov test is based on three assumptions, one being that clasts have a random orientation (Shipunov et al., 1998). While this assumption is usually true for well-rounded pebbles and boulders, it is not necessarily true for breccia clasts that may have undergone minor amounts of rotation. Another assumption (Shipunov et al., 1998) is that a possible remagnetization direction is known. The approach of using some arbitrary direction as a possible secondary direction, as we did with the south-down component, instead of a known secondary overprint, is less than ideal and may be erroneous (Shipunov et al., 1998).

In order to illustrate the statistical distinctiveness of the two distributions (i.e., the characteristic components from parent lithology vs. pillow fragments) we choose to test for a common mean (Tauxe et al., 2009). Despite the large uncertainty of the mean for the characteristic components seen in pillow fragments, we can illustrate that the mean from the parent pillow lava samples is significantly different at the 95% level (Fig. 5). We interpreted this result as a positive intraformational conglomerate test and suggest that the Shipunov's test and Watson test for randomness result in Type-1 statistical errors due to limited rotation of pillow clasts during the formation of the hyaloclastite, and/or delayed remanence lock-in in lava clasts or partial remagnetization during subsequent extrusion of overlying lava flows.

### 3.4. Interpretation of results

#### 3.4.1. Secondary A component

A north-down remanence direction was identified in samples from three sampling sites (Table 2) within a relatively narrow temperature range between 300 °C and 375 °C, but sometimes as high as 450 °C. A mean declination = 349.7° and inclination = 62.0° translates to a paleopole at 16.7°N, 015.7°E with $A_{95}$ = 15.7°. A negative conglomerate test for this component in clasts from a blocky flow-top breccia implies that it is a secondary component acquired after extrusion of the Allanridge Formation lavas.

Comparison with known poles from the Kaapvaal craton (de Kock et al., 2006) suggests either ~2.0 Ga or 1.8–1.9 Ga as possible times of acquisition of this overprint (Fig. 6). The Bushveld complex (Fig. 2) intruded at this time (Buick et al., 2001) and the Vredefort impact is dated at 2023 Ma (Kamo et al., 1996). Both of these events have been implicated as potential sources of widespread remagnetization on the central Kaapvaal craton (Evans et al., 2002; Layer et al., 1988). Extensive intraplate magmatism also occurred during the development of the Waterberg and Soutpansberg Groups at ~1.9 Ga and ~1.8 Ga (Hanson et al., 2004). The Trompsburg intrusion, which is responsible for the so-called Trompsburg anomaly (Fig. 2), has also yielded a 1.9 Ga age (Maier et al., 2003). The restricted occurrence of the north-down overprint, however, attests to the generally undisturbed preservation of the Ventersdorp succession in the Kimberley region and invites further paleomagnetic study in this relatively pristine area.

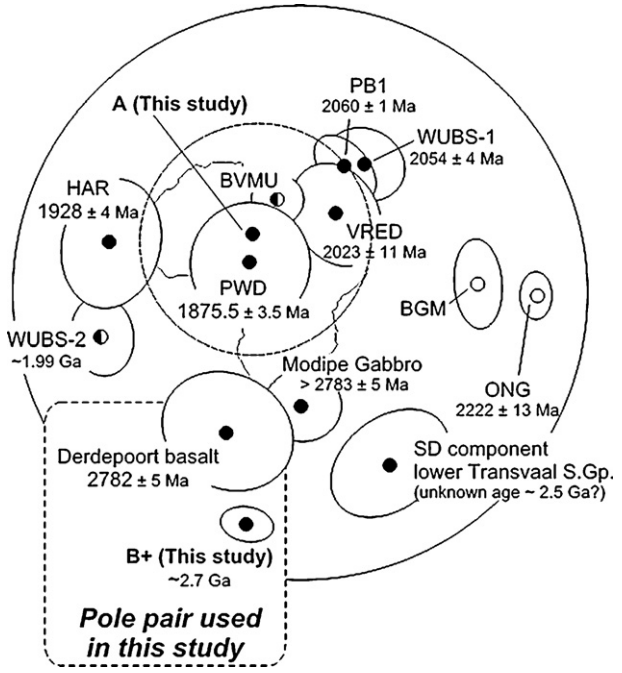


**Fig. 6.** Comparison of the paleomagnetic poles described by the A and B+ components identified in this study with known paleopoles from the Kaapvaal craton (See de Kock et al., 2006, 2009 for pole references. The Modipe Gabbro pole is taken from Evans and McElhinny, 1966.) Abbreviations: SD = south-down component VGP from the Lower Transvaal Supergroup; ONG = Ongeluk lava paleopole; BGM = Basal Gamagara-Mapedi Formation VGP; PB1 = Palaborwa Group 1 paleopole; WUBS-1 = Waterberg unconformity-bounded sequence 1 paleopole; VRED = Vredefort impact structure VGP; BVMU = Bushveld Main and Upper Zones paleopole; WUBS-2 = Waterberg unconformity-bounded sequence 2 paleopole; HAR = Hartley Lava VGP; PWD = Post-Waterberg Dolerites paleopole.

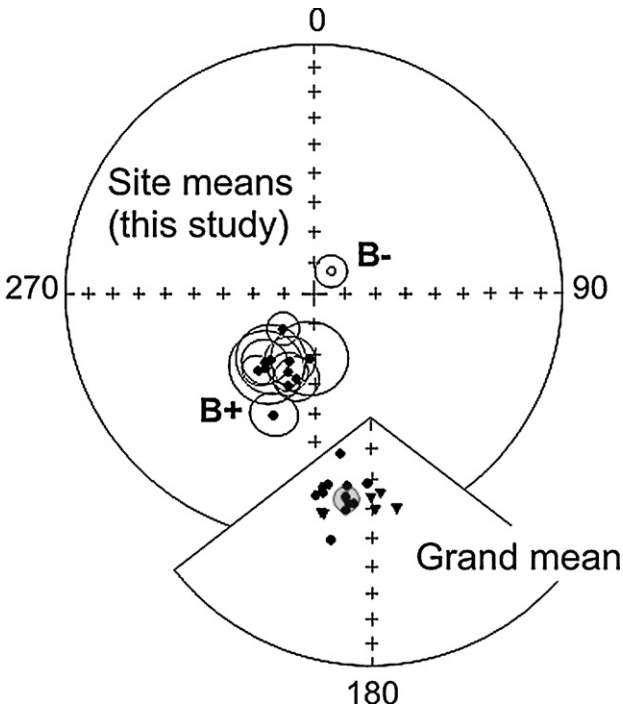


**Fig. 7.** Equal area projection of the B+ and B− component site means found during this study and grand mean of our B+ characteristic component combined with that of Strik et al. (2007). Solid = lower hemisphere, open = upper hemisphere, circles = this study, triangles = components from (Strik et al., 2007). Ellipses are cones of 95% confidence associated with component means. Grand mean confidence is shaded.

*3.4.2. Primary B+ and B− component*

In addition to a positive conglomerate test, the results from one sampling site suggest dual polarity magnetizations. Since no stability field tests were conducted to evaluate the acquisition age of B− we conservatively use only those sites that reliably recorded B+ ($N = 11$) to compute a mean with declination = 203.9°, inclination 62.5°, $k$-parameter = 88.6 and $\alpha_{95} = 4.9°$ (Fig. 7). This corresponds to a paleomagnetic pole at −65.6°S and 339.5°E with $K = 50.5$ and $A_{95} = 6.5°$. The age of the pole is constrained to the time of the Allanridge's eruption (i.e., ~2.70 Ga), and it represents a significant improvement of existing age constraints from pre-Permian to Neoarchean (Strik et al., 2007). Our data can be combined with the work of Strik and colleagues (2007) for the calculation of a grand mean from 18 sampling sites (Fig. 7). Since bulk demagnetization techniques were employed in the pre-1980 studies, and the complete removal of secondary overprints cannot be guaranteed, we chose to exclude them from our calculation. The corresponding pole position (69.8°S, 345.6°E, $K = 36.7$, $A_{95} = 5.8°$) has a reliability criterion (Van der Voo, 1990) of $Q = 6$ (lacking only dual polarity, for which we have preliminary evidence, but conservatively omit) and does not share any similarities with known Neoarchean-Paleoproterozoic Kaapvaal craton poles (Fig. 6) (de Kock et al., 2006, 2009).

## 4. Discussion

*4.1. Pole-pair comparison and reconstruction*

Following a method (Evans and Pisarevsky, 2008) of calculating the great-circle arc distance between the 2.78 Ga and 2.70 Ga Kaapvaal poles and comparing that to the great-circle distance between similarly aged poles from the Pilbara, we show that common motion between these cratons is allowable for this time interval. The method constrains the relative longitudinal separation between the cratons. An alternative possibility, due to polarity ambiguity, could reconstruct the cratons in opposite hemispheres, but this detracts from the similarities that originally prompted the Vaalbara hypothesis. Unlike previously suggested reconstructions, all of which fail to align the two pairs of paleomagnetic poles from 2.78 and 2.70 Ga (Fig. 8a–c), our new reconstruction overlaps the two paleopole pairs and places the Pilbara immediately to the northwest of the present-day Kaapvaal craton in a Kaapvaal reference frame (Fig. 8d). It aligns paleogeographic features on both cratons from as early as 2.9–2.8 Ga, and as late as ~2.1 Ga. There is still considerable room for manoeuvring the Kaapvaal relative to the Pilbara craton, given the large uncertainties still surrounding the K1 pole. This allows for a large number of viable reconstructions, all equally possible, and all sharing the constant placement of the Pilbara craton somewhere towards the northwest of the Kaapvaal craton (Fig. 8d). Our preferred fit ensures continuity between the two cratons by a crossing of the P1–P2 and K1–K2 paths rather than paralleling apparent polar wander paths, and by allowing a slight mismatch between the K1 and P1 poles (Fig. 8d). This is deemed allowable given the large uncertainties associated with the K1 pole and the ~10 million year age difference between the K1 and P1 poles.

*4.2. Vaalbara through time*

Pilbara must undergo an anticlockwise rotation of about 90° and significant displacement between 2.83 Ga and 2.78 Ga if the Zegers fit is valid at 2.83 Ga. Two discrete, but extensive magmatic episodes, one between 2954 Ma and 2930 Ma and another between 2890 Ma and 2830 Ma, has been identified in the northern Pilbara craton (Van Kranendonk et al., 2007). These events, which the

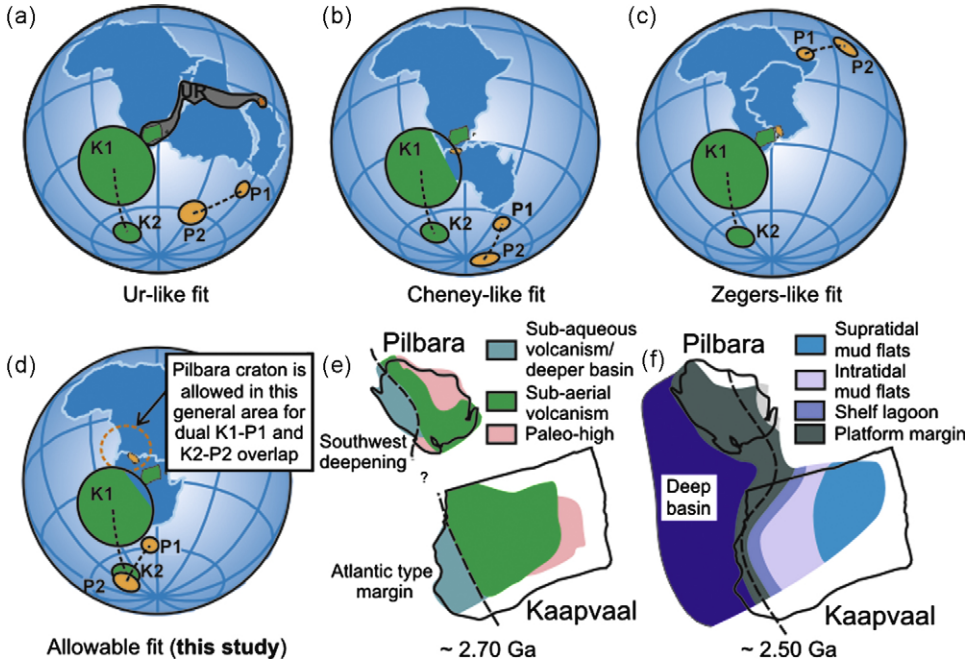


**Fig. 8.** 2.78 Ga and 2.70 Ga pole-pair comparison. All reconstructions are in a present Kaapvaal reference frame and centred on 30°S and 30°E. In global views the Kaapvaal and the Grunehogna cratons are indicated in green, whereas the Pilbara craton is orange. Kaapvaal poles (green): K1 = 2782 ± 5 Ma Derdepoort Basalt pole (Wingate, 1998), K2 = ~2.7 Ga Allanridge Formation pole (this study). Pilbara poles (Strik et al., 2003) in orange: P1 = 2772 ± 2 Ma Pilbara Flood basalts Package 1, P2 = 2717 ± 2 Ma Pilbara Flood basalts Package 8–10. Angular distances: K1–K2 = 31.8 ± 23.3°, P1–P2 = 24.7 ± 16.2°. (a) Ur-like fit produces misalignment of pole pairs. Pilbara was rotated into a Pangean position about an Euler pole at 29.1°S, 57.2°W through an anticlockwise angle of 54.1°. (b) Cheney fit with the Pilbara south of Kaapvaal does not result in pole overlap: Pilbara is rotated about an Euler pole at 71.7°N, 40.6°E through an angle of −85.0°. (c) Zegers fit was originally suggested for 2.83 Ga old poles, but a similar fit causes large separation between the 2.78 Ga and 2.70 Ga pole pairs. For the Zegers fit to be valid at 2.83 Ga, the Pilbara craton has to undergo a near 90° anticlockwise rotation and significant displacement before 2.78 Ga. Rotation parameters for the Pilbara craton: 39.3°N, 102.9°W through an angle of −156.9°. (d) Overlap of similarly aged poles is achieved by rotating the Pilbara 93.2° about an Euler pole at 59.0°S, 251.5°E, bringing it in close and to the northwest of Kaapvaal. *Note*: Pilbara is allowed in a restricted area northwest of Kaapvaal given the pole constraints, but we prefer a tight fit based on geological constraints. (e) Paleogeography and volcanic facies distribution at ~2.70 Ga superimposed onto reconstruction (d). (f) Paleogeography and sedimentary facies distribution at ~2.50 Ga superimposed onto reconstruction (d). Dashed curves in e and f indicate paleocontinental shelf-slope boundaries. (For interpretation of the references to colour in this figure legend, the reader is referred to the web version of the article.)

Zegers fit (Fig. 8c) predicts to be represented in the eastern Kaapvaal, have thus far gone unrecognized (Eglington and Armstrong, 2004; Poujol et al., 2003) – during these times the eastern and central parts of the craton experienced a period of magmatic quiescence. The younger, western and northern parts of Kaapvaal, however, share voluminous plutonism at 2.88–2.82 Ga with the northern Pilbara Kurrana Terrane (Eglington and Armstrong, 2004; Schmitz et al., 2004) and possibly with the Sylvania inlier (southwestern Pilbara). No precise ages exist for basement rocks from the Sylvania inlier, but Rb-Sr ages approximately ~2.8 Ga (Tyler, 1991), and a minimum age is provided by ~2.75 Ga NNE trending dikes (Wingate, 1999). Furthermore, in our reconstruction, the trends of greenstone belts of the Sylvania inlier align with those of the Kraaipan and Amalia greenstone belts of Kaapvaal, suggesting that the cratons shared a similar history since 3.2–3.0 Ga (Poujol et al., 2003).

The parallel development of Neoarchean volcano-sedimentary sequences, which constitutes the foundation of the Vaalbara hypothesis, provides geological piercing points for our reconstruction. Both this study and the Cheney fit align major structural trends throughout the development of the two sequences, but paleomagnetic data contradict the Cheney fit (Fig. 8a). Facies in the upper Fortescue Group suggest a deepening of the Fortescue basin toward the west and a NW-SE stretching paleoshoreline when the Pilbara is placed to the northwest of Kaapvaal (Thorne and Trendall, 2001). Seismic reflectors, above and below the Allanridge Formation, reveal a similar westward deepening of the Ventersdorp basin (Tinker et al., 2002) (Fig. 8e).

The westward deepening and general NW-SE paleoshoreline were maintained throughout deposition of the Hamersley Group and the Vryburg Formation-lower Transvaal Supergroup (Beukes, 1987; McConchie, 1984; Morris and Horwitz, 1983). Superimposing geochronological, paleogeographical and structural information from these successions onto the proposed reconstruction illustrate this (Fig. 8f). Simultaneous deposition of carbonates and iron-formation during this time further supports parallel basin development (Nelson et al., 1999; Pickard, 2003). A single Transvaal-Hamersley basin at ~2.5 Ga, which is representative of only a small portion of the Earth's surface, should be considered when evaluating the secular trends in chemical sedimentation, stable isotope signatures, and paleoclimate proxies.

We cautiously evaluate the existence of Vaalbara after ~2.5 Ga. After the ~2.7 Ga pole (this paper), the paleopole record from the Kaapvaal resumes only at 2.22 Ga (Evans et al., 1997), from when on it is well defined until ~1.87 Ga (de Kock et al., 2006). The equivalent Pilbaran record is poor, and the only pole comparison that can be made is at ~2.0 Ga or ~1.8 Ga, depending on the age assigned to iron ores of the Hamersley province (de Kock et al., 2008). Following the method of comparing great-circle distances between successive poles, it can be shown that either age assignment is unsupportive of our Vaalbara model. This implies either that Vaalbara fragmented by ~2.0 Ga, or if the ~1.8 Ga age is preferred, that the Vaalbara connection is possible at 2.0 Ga, but unlikely thereafter. Kaapvaal experienced compression before ca. 2.1 Ga (Beukes et al., 2002), which was responsible for the development of long-wavelength N-S axial-folds. Riebeckite is associated with the axial zones of these folds (Button, 1979). On the Pilbara craton the ca. 2208–2031 Ma (Müller et al., 2005) Ophthalmian orogeny was responsible for the development of E-W trending fold

axes. Here too, Riebeckite is associated with the folds (Krapez et al., 2003). A clockwise rotation of Pilbara, as our reconstruction implies, brings the fold axes of the cratons into rough alignment. Shared histories thus support our Vaalbara model up to ~2.1 Ga.

## 5. Conclusions

A good match between the apparent polar wander paths of the Kaapvaal and Pilbara cratons for the period 2.78–2.70 Ga together with strikingly similar geological features (e.g., lithostratigraphy, geochronology, structures, etc.) provide the best evidence thus far for the existence of Vaalbara during the late Neoarchean and early Paleoproterozoic eras. Improved paleomagnetic data paired with improved age constraints from units like the Derdepoort, Kanye and Lobatse volcanics; the Modipe Gabbro; Allanridge Formation and Vryburg Formation as well as the numerous dike swarms exposed especially on the eastern part of the Kaapvaal craton can help constrain the configuration of Vaalbara significantly. The currently available paleomagnetic data constrain the position of the Pilbara craton in close immediate proximity towards the northwest of the Kaapvaal craton in a present-day Kaapvaal reference frame. This reconstruction provides the oldest example, and the only Archean instance, of paleomagnetic reconstruction between continental blocks in terms of both paleolatitude and relative longitude. It may also require a significant reappraisal of previous paleoenvironmental conclusions concerning the Archean-Paleoproterozoic boundary in the Hamersley and Transvaal basins. Our reconstruction implies that any detailed datasets coming from these well-preserved stratigraphies represent one basin, in one location on the 2.7–2.2 Ga Earth.

## Acknowledgements

The South African National Research Foundation and the Agouron Institute for Geobiology supported this study. D.A.D.E. acknowledges support of the David and Lucile Packard Foundation. We would like to thank Wouter Bleeker, Joe Meert and Lisa Tauxe for their critical readings of the manuscript.

## References

Armstrong, R.A., Compston, W., Retief, E.A., Williams, I.S., Welke, H.J., 1991. Zircon ion microprobe studies bearing on the age and evolution of the Witwatersrand triad. Precambrian Research 53, 243–266.

Barton, J.M.J., Blignaut, E., Salnikova, E.B., Kotov, A.B., 1995. The stratigraphical position of the Buffelsfontein Group based on field relationships and chemical and geochronological data. South African Journal of Geology 98, 386–392.

Beukes, N.J., 1987. Facies relations, depositional environments and diagenesis in a major Early Proterozoic stromatolitic carbonate platform to basinal sequence, Campbellrand Subgroup, Transvaal Supergroup, Southern Africa. Sedimentary Geology 54, 1–46.

Beukes, N.J., Dorland, H.C., Gutzmer, J., Nedachi, M., Ohmoto, H., 2002. Tropical laterites, life on land, and the history of atmospheric oxygen in the Paleoproterozoic. Geology 30 (6), 491–494.

Blake, T.S., Buick, R., Brown, S.J.A., Barley, M.E., 2004. Geochronology of a Late Archaean flood basalt province in the Pilbara Craton, Australia: constraints on basin evolution, volcanic and sedimentary accumulation, and continental drift rates. Precambrian Research 133, 143–173.

Boger, S.D., Wilson, C.J.L., Fanning, C.M., 2001. Early Paleozoic tectonism within the East Antarctic craton: the final suture between east and west Gondwana? Geology 29, 463–466.

Buick, I.S., Maas, R., Gibson, R., 2001. Precise U-Pb titanite age constraints on the emplacement of the Bushveld Complex, South Africa. Journal of the Geological Society, London 158, 3–6.

Button, A., 1979. Transvaal and Hamersley Basins—review of basin development and mineral deposits. Minerals Science and Engineering 8, 262–290.

Cheney, E.S., 1990. Evolution of the "Southwestern" continental margin of Vaalbara, Extended Abstracts Geocongress'90. Geological Society of South Africa, Cape Town, pp. 88–91.

Cheney, E.S., 1996. Sequence stratigraphy and plate tectonic significance of the Transvaal succession of southern Africa and its equivalent in Western Australia. Precambrian Research 79, 3–24.

Cogné, J.P., 2003. PaleoMac: a Macintosh (application for reconstructions. Geochemistry Geophysics Geosystems 4, 1007, doi:10.1029/2001GC000227.

Collins, A.S., Pisarevsky, S.A., 2005. Amalgamating eastern Gondwana: the evolution of the Circum-Indian Orogens. Earth-Science Reviews 71, 229–270.

Crow, C., Condie, K.C., 1988. Geochemistry and origin of late Archean volcanics from the Ventersdorp Supergroup, South Africa. Precambrian Research 42 (1–2), 19–37.

Council for Geoscience, 1997. Geological Map of the Republic of South Africa and the Kingdoms of Leshoto and Swaziland. Council for Geoscience, Pretoria, 1:1 000 000.

De Beers, 1998. Aeromagnetic map. In: Ayers, N.P., Hatton, C.J., Quadling, K.E., Smith, C.D. (Eds.), Update on the Distribution in Time and Space of Southern African Kimberlites.

de Kock, M.O., 2007. Paleomagnetism of selected Neoarchean-Paleoproterozoic cover sequences on the Kaapvaal craton and implications for Vaalbara. Unpublished Ph.D. Thesis. University of Johannesburg, Johannesburg, 276 pp.

de Kock, M.O., Evans, D.A.D., Dorland, H.C., Beukes, N.J., Gutzmer, J., 2006. Paleomagnetism of the lower two unconformity-bounded sequences of the Waterberg Group, South Africa: towards a better-defined apparent polar wander path for the Paleoproterozoic Kaapvaal Craton. South African Journal of Geology 109 (1), 157–182.

de Kock, M.O., Evans, D.A.D., Gutzmer, J., Beukes, N.J., Dorland, H.C. (Eds.), 2008. Origin and Timing of BIF-hosted High-grade Hard Hematite Deposits—A Paleomagnetic Approach. BIF-related High-grade Iron Mineralization, Reviews in Economic Geology, vol. 15. Society for Economic Geologists, pp. 49–71.

de Kock, M.O., Evans, D.A.D., Kirschvink, J.L., Beukes, N.J., Rose, E., Hilburn, I., 2009. Paleomagnetism of a Neoarchean-Paleoproterozoic carbonate ramp and carbonate platform succession (Transvaal Supergroup) from surface outcrop and drill core, Griqualand West region, South Africa. Precambrian Research 169, 80–99.

Eglington, B.M., Armstrong, R.A., 2004. The Kaapvaal Craton and adjacent orogens, southern Africa: a geochronological database and overview of the geological development of the craton. South African Journal of Geology 107, 13–32.

England, G.L., et al., 2001. SHRIMP U-Pb ages of diagenetic and hydrothermal xenotime from the Archean Witwatersrand Supergroup of South Africa. Terra Nova 13, 360–367.

Evans, D.A., Beukes, N.J., Kirschvink, J.L., 1997. Low-latitude glaciation in the Palaeoproterozoic era. Nature 386, 262–266.

Evans, D.A.D., Beukes, N.J., Kirschvink, J.L., 2002. Paleomagnetism of a lateritic paleoweathering horizon and overlying Paleoproterozoic red beds from South Africa: implications for the Kaapvaal apparent polar wander path and a confirmation of atmospheric oxygen enrichment. Journal of Geophysical Research 107 (No. BN12, 2326), doi:10.1029/2001JB000432.

Evans, D.A.D., Pisarevsky, S.A., 2008. Plate tectonics on the early Earth?—weighing the paleomagnetic evidence. In: Condie, K., Pease, V. (Eds.), When did Plate Tectonics Begin? Geological Society of America, pp. 249–263.

Evans, M.E., McElhinny, M.W., 1966. The Paleomagnetism of the Modipe Gabbro. Journal of Geophysical Research 70, 6053–6063.

Fitzsimons, I.C.W., 2000. Grenville-age basement provinces in East Antarctica: evidence for three seperate collisional orogens. Geology 28, 879–882.

Geological Survey Department Lobatse, 1984. Geological Map of the Republic of Botswana, 1: 1000 000.

Grobler, D.F., Walraven, F., 1993. Geochronology of Gabarone Granite Complex extensions in the area north of Mafikeng, South Africa. Chemical Geology 105, 319–337.

Hanson, R.E., et al., 2004. Coeval large-scale magmatism in the Kalahari and Laurentian cratons during Rodinia assembly. Science 304, 1126–1129.

Henthorn, D.I., 1972. Paleomagnetism of the Witwatersrand Triad Republic of South Africa and related topics. Unpublished PhD Thesis, The University of Leeds, 103 pp.

Jacobs, J., Thomas, R.J., 2004. Himalayan-type indenter-escape tectonics model for the south part of the late Neoproterozoic-early Paleozoic East African-Antarctic orogen. Geology 32, 721–724.

Jones, C.H., 2002. User-driven integrated software lives: "Paleomag" Paleomagnetic analysis on the Macintosh™. Computers and Geosciences 28, 1145–1151.

Jones, D.L., Walford, M.E.R., Gifford, A.C., 1967. A paleomagnetic result from the Ventersdorp Lavas of South Africa. Earth and Planetary Science Letters 2, 155–158.

Jones, D.L., Bates, M.P., Li, Z.X., Corner, B., Hodgkinson, G., 2003. Palaeomagnetic results from the ca. 1130 Ma Borgmassivet intrusions in the Ahlmannryggen region of Dronning Maud Land, Antarctica, and tectonic implications. Tectonophysics 375, 247–260.

Kamo, S.L., Reimold, W.U., Krogh, T.E., Colliston, W.P., 1996. A 2.023 Ga age for the Vredefort impact event and a first report of shock metmorphosed zircons in pseudotachylitic breccias and granophyre. Earth and Planetary Science Letters 144, 369–387.

Kaufman, A.J., et al., 2007. Late Archean biospheric oxygenation and atmospheric evolution. Science 317, 1900–1903.

Kirschvink, J.L., 1980. The least squares line and plane and the analysis of palaeomagnetic data. Geophysical Journal of the Royal Astronomical Society 62, 699–718.

Krapez, B., Barley, M.E., Pickard, A.L., 2003. Hydrothermal and resedimented origin of the precursor sediments to banded iron formation: sedimentological evidence from the Early Paleoproterozoic Brockman Supersequence of Western Australia. Sedimentology 50, 979–1011.

Layer, P.W., Kröner, A., McWilliams, M., Clauer, N., 1988. Regional magnetic overprinting of Witwatersrand Supergroup sediments, South Africa. Journal of Geophysical Research 93 (B3), 2191–2200.

Maier, W.D., Peltonen, P., Grantham, G., Mänttäri, I., 2003. A new 1.9 Ga age for the Trompsburg intrusion, South Africa. Earth and Planetary Science Letters 212, 351–360.
McConchie, D., 1984. A depositional environment for the Hamersley Group: palaeogeography and geochemistry. In: Muhling, J.R., Groves, D.I., Blake, T.S. (Eds.), Archean & Proterozoic Basins of the Pilbara, Western Australia: Evolution & Mineralization Potential. University Extention, The University of Western Australia, Nedlans, Western Australia, pp. 144–195.
Meert, J.G., 2003. A synopsis of events related to the assembly of eastern Gondwana. Tectonophysics 362, 1–40.
Mondal, S., Piper, J.D.A., Hunt, I., Banyopadhyay, G., Basu Mallik, S., 2009. Palaeomagnetic and rock magnetic study of charnockites from Tamil Nadu, India, and the 'Ur' protocontinent in Early Palaeoproterozoic times. Journal of Asian Earth Science 34, 493–506.
Moore, M., Davis, D.W., Robb, L.J., Jackson, M.C., Grobler, D.F., 1993. Archean rapakivi granite-anorthosite-rhyolite complex in the Witwatersrand basin hinterland, southern Africa. Geology 21, 1031–1034.
Morris, R.C., Horwitz, R.C., 1983. The origin of the iron-formation-rich Hamersley Group of Western Australia—deposition on a platform. Precambrian Research 21, 273–297.
Mukherjee, A., Das, S., 2002. Anorthosites, granulites and the supercontinent cycle. Gondwana Research 5 (1), 147–156.
Müller, S.G., Krapez, B., Barley, M.E., Fletcher, I.R., 2005. Giant iron-ore deposits of the Hamersley province related to the breakup of Paleoproterozoic Australia: new insights from in-situ SHRIMP dating of baddeleyite from mafic intrusions. Geology 33 (7), 577–580.
Nelson, D.R., Trendall, A.F., Altermann, W., 1999. Chronological correlations between the Pilbara and Kaapvaal cratons. Precambrian Research 97, 165–189.
Nelson, D.R., Trendall, A.F., De Laeter, J.R., Grobler, N.J., Fletcher, I.R., 1992. A comparative study of the geochemical and isotopic systematics of late Archaean flood basalts from the Pilbara and Kaapvaal cratons. Precambrian Research 54 (2–4), 231–256.
Pickard, A., 2003. SHRIMP U-Pb zircon ages for the Palaeoproterozoic Kuruman Iron Formation, Northern Cape Province, South Africa: evidence for simultaneous BIF deposition on Kaapvaal and Pilbara Cratons. Precambrian Research 125, 275–315.
Poujol, M., Kiefer, R., Robb, L.J., Anhaeusser, C.R., Armstrong, R.A., 2005. New U-Pb data on zircons from the Amalia greenstone belt Southern Africa: insights into the Neoarchean evolution of the Kaapvaal Craton. South African Journal of Geology 108 (3), 317–332.
Poujol, M., Robb, L.J., Anhaeusser, C.R., Gericke, B., 2003. A review of the geochronological constraints on the evolution of the Kaapvaal Craton, South Africa. Precambrian Research 127, 181–213.
Rogers, J.J.W., 1996. A history of the continents in the past three billion years. The Journal of Geology 104, 91–107.
Rogers, J.J.W., Santosh, M., 2003. Supercontinents in earth history. Gondwana Research 6 (3), 357–368.
Schmitz, M.D., Bowring, S.A., De Wit, M.J., Gartz, V., 2004. Subduction and terrane collosion stabilize the western Kaapvaal craton tectosphere 2.9 billion years ago. Earth and Planetary Science Letters 222, 363–376.
Shipunov, S.V., Muraviev, A.A., Bazhenov, M., 1998. A new conglomerate test in palaeomagnetism. Geophysics Journal International 133, 721–725.
Strik, G., Blake, T.S., Zegers, T.E., White, S.H., Langereis, C.G., 2003. Palaeomagnetism of flood basalt in the Pilbara Craton, Western Australia: late Archaean continental drift and the oldest known reversal of the geomagnetic field. Journal of Geophysical Research 108, doi:10.1029/2003JB002475.
Strik, G., De Wit, M.J., Langereis, C.G., 2007. Palaeomagnetism of the Neoarchaean Pongola and Ventersdorp Supergroups and an appraisal of the 3.0–1.9 Ga apparent polar wander path of the Kaapvaal Craton, Southern Africa. Precambrian Research 153, 96–115.
Tauxe, L., Butler, R.F., Banerjee, S., Van der Voo, R., 2009. Essentials of Paleomagnetism. University of California, Berkeley.
Thorne, A.M., Trendall, A.F., 2001. Geology of the Fortescue Group, Pilbara Craton, Western Australia, Bulletin 144. Western Australia Geological Survey, 249 pp.
Tinker, J., De Wit, M.J., Grotzinger, J., 2002. Seismic stratigraphic constraints on Neoarchean-Paleoproterozoic evolution of the western margin of the Kaapvaal Craton, South Africa. South African Journal of Geology 105, 107–134.
Trendall, A.F., 1968. Three great basins of Precambrian iron formation deposition: a systematic comparison. Geological Society of America Bulletin 79, 1527–1533.
Tyler, I.M., 1991. The Geology of the Sylvania Inlier and the Southeast Hamersly Basin. Bulletin, vol. 138. Geological Survey of Western Australia, Perth, 108 pp.
Van der Voo, R., 1990. The reliability of paleomagnetic data. Tectonophysics 184, 1–9.
Van Kranendonk, M.J., Smithies, R.H., Hickman, A.H., Champion, D.C., 2007. Review: secular tectonic evolution of Archean continental crust: interplay between horizontal and vertical processes in the formation of the Pilbara Craton, Australia. Terra Nova 19, 1–38.
Wingate, M.T.D., 1998. A palaeomagnetic test of the Kaapvaal–Pilbara (Vaalbara) connection at 2.78 Ga. South African Journal of Geology 101 (4), 257–274.
Wingate, M.T.D., 1999. Ion microprobe baddeleyite and zircon ages for Late Archaean mafic dykes of the Pilbara craton, Western Australia. Australian Journal of Earth Sciences 46 (4), 493–500.
Zegers, T.E., De Wit, M.J., Dann, J., White, S.H., 1998. Vaalbara, Earth's oldest assembled continent? A combined structural, geochronological, and palaeomagnetic test. Terra Nova 10, 250–259.
Zhao, G., Sun, M., Wilde, S.A., Sanzhong, L., Jian, Z., 2006. Some key issues in reconstructions of Proterozoic supercontinents. Journal of Asian Earth Sciences 28, 3–19.